



NOTE

Internal Medicine

Findings of contrast-enhanced ultrasonography with Sonazoid for cholangiocellular adenoma in three dogs

Masahiro TAMURA¹⁾, Kensuke NAKAMURA²⁾, Tatsuyuki OSUGA³⁾, Genya SHIMBO³⁾, Noboru SASAKI¹⁾, Keitaro MORISHITA³⁾, Hiroshi OHTA¹⁾ and Mitsuyoshi TAKIGUCHI¹⁾*

¹⁾Laboratory of Veterinary Internal Medicine, Department of Veterinary Clinical Sciences, Graduate School of Veterinary Medicine, Hokkaido University, Hokkaido 060-0818, Japan

²⁾Organization for Promotion of Tenure Track, University of Miyazaki, Miyazaki 889-2192, Japan

³⁾Veterinary Teaching Hospital, Graduate School of Veterinary Medicine, Hokkaido University, Hokkaido 060-0819, Japan

ABSTRACT. Contrast-enhanced ultrasonography (CEUS) is useful to distinguish benign and malignant focal liver lesions in dogs. Cholangiocellular adenoma is an extremely rare benign tumor in dogs and has not been examined using CEUS with Sonazoid. The aim of this study was to describe findings of CEUS with Sonazoid in three dogs with cholangiocellular adenoma. All three dogs showed contrast defects in the Kupffer phase and these findings mimicked malignant neoplasia during the Kupffer phase. Moreover, all dogs showed early washout and hypoechoic lesions relative to the surrounding normal liver parenchyma in the portal phase. To our knowledge, this is the first study to report that CEUS findings of cholangiocellular adenoma with Sonazoid mimicked malignancy in three dogs.

KEY WORDS: cholangiocellular adenoma, contrast-enhanced ultrasound, dog, Kupffer phase, Sonazoid

J. Vet. Med. Sci.

81(8): 1104–1108, 2019

doi: 10.1292/jvms.19-0116

Received: 27 February 2019

Accepted: 24 April 2019

Advanced Epub: 27 June 2019

Contrast-enhanced ultrasonography (CEUS) is a relatively recent development in imaging that takes advantage of microbubble technology and improves the visualization and characterization of anatomical structures and lesions. Previous studies described the usefulness of CEUS in terms of distinguishing benign and malignant liver tumors in dogs [8, 10, 12]. Second-generation contrast agents, such as SonoVue[®] (Bracco Diagnostics, Inc., Milan, Italy) and Sonazoid[®] (Daiichi-Sankyo Co., Ltd., Tokyo, Japan), are now commercially available in North America, Europe, and Asia. SonoVue, consisting of sulfur hexafluoride (SF₆) within a phospholipid shell, allows the visualization of small vessels and microvascular perfusion in capillary beds and tumors. The administration of SonoVue provides three phases in the liver, which has a dual blood supply from the hepatic artery and portal vein: the vascular (arterial and portal) phase and late phase. The late phase continues until the gas dissolves and is eliminated in expired air [5, 14]. Sonazoid, consisting of perfluorobutane within a hydrogenated egg phosphatidylserine shell, also provides the vascular (arterial and portal) phase, similar to SonoVue. Additionally, Sonazoid has the unique feature of being phagocytosed by Kupffer cells in the reticuloendothelial system of the liver. Therefore, Sonazoid enables parenchyma-specific liver imaging, called the Kupffer phase. Previous studies on dogs and human patients reported that malignant lesions containing few or no Kupffer cells were clearly delineated as contrast defects in Kupffer phase [8, 10, 13, 14].

Cholangiocellular adenoma is an extremely rare benign tumor in dogs [2]. A previous study initially reported that a dog with cholangiocellular adenoma showed findings mimicking malignant neoplasia using CEUS with SonoVue even though it was a benign tumor [1]. However, cholangiocellular adenoma in dogs has not been examined using Sonazoid and it still remains unclear whether CEUS with Sonazoid will show findings that mimic malignant neoplasia in dogs with cholangiocellular adenoma. We herein report findings on arterial, portal, and Kupffer phase images of CEUS with Sonazoid in three dogs histopathologically diagnosed with cholangiocellular adenoma.

A retrospective case series study was performed at the Hokkaido University Veterinary Teaching Hospital. The medical records of dogs diagnosed with cholangiocellular adenoma between October 2014 and April 2018 were reviewed. Inclusion criteria were as follow: (1) liver nodules detected using conventional abdominal ultrasonography and were subjected to CEUS before surgery; (2) a

*Correspondence to: Takiguchi, M.: mtaki@vetmed.hokudai.ac.jp

©2019 The Japanese Society of Veterinary Science



This is an open-access article distributed under the terms of the Creative Commons Attribution Non-Commercial No Derivatives (by-nc-nd) License. (CC-BY-NC-ND 4.0: <https://creativecommons.org/licenses/by-nc-nd/4.0/>)

definitive histological diagnosis of cholangiocellular adenoma by a single board-certified veterinary pathologist (Y.K.) according to the WSAVA criteria [2].

Regarding the distinction between benign and malignant lesions, we performed CEUS preoperatively without sedation on all dogs. US equipment (Aplio 500, Canon Medical Systems, Tochigi, Japan) using a 5–11 MHz broadband linear transducer (PVT-704 AT, Canon Medical Systems, Tochigi, Japan) was optimized for a low mechanical index of 0.15–0.21, frame rate of 15–20 frames per second, Doppler gain of 80, and dynamic range of 45. CEUS was performed by two investigators (M.T., K.N., with at least 5 years' experience of abdominal ultrasound). All dogs had a 22-gauge intravenous catheter inserted into the cephalic vein with a 21-gauge butterfly catheter. Perfusion imaging was evaluated after contrast agent (Sonazoid, 0.01 ml/kg) had been intravenously injected through the catheter, followed by flushing with 3 ml of heparinized normal saline. The dose of microbubbles was selected according to our previously described methods [9]. CEUS imaging was obtained as cine-loops in the digital imaging and communication in medicine (DICOM) format. Based on a previous study on dogs with liver tumors [8, 10], we evaluated the contrast phase: We assessed findings from 0 to 15 sec after the injection as the arterial phase, 30 sec after the injection as the portal phase, and at least 7 min after the injection as the Kupffer phase. Based on previous studies on dogs and humans, we evaluated the vascular pattern of liver lesions in the arterial phase [8]. The echogenicities of liver lesions in all phases were evaluated as hyperechoic, isoechoic, and hypoechoic lesions relative to the surrounding normal parenchyma.

Inclusion criteria in the present study were fulfilled by three dogs: Case 1 was a 13-year-old, 7.4 kg, castrated male Miniature Dachshund; Case 2 was an 11-year-old, 7.12 kg, spayed female Scottish Terrier; Case 3 was a 12-year-old, 2.78 kg, spayed female Toy Poodle. Each dog underwent a laparotomy. The affected liver lobes including each nodule were removed using liver lobectomy techniques based on surgeon's preference. All resected tissues were fixed in formalin and embedded in paraffin, and the sections were stained with hematoxylin and eosin. The histopathological examination showed that each mass had a ductular and papillary growth pattern and consisted of well-differentiated cuboidal epithelium with cystic structures. Cuboidal epithelial cells had a moderate amount of pale eosinophilic cytoplasm, nuclei were round to oval and basally oriented. The epithelium was single layer and a mitotic figure is almost never observed. The mass included no structures and cells derived from the hepatic parenchyma. Based on these findings, each mass was diagnosed as cholangiocellular adenoma (Fig. 1).

Case 1 had a focal and hyperechoic large liver nodule with ill-defined margins. The nodule had a maximal diameter of 7.8 cm and was detected in the left division of the liver. The nodule contained multiple cystic regions (Fig. 2A–C). The remaining liver parenchyma had a normal appearance. In the arterial phase under CEUS, the nodule showed a dysmorphic vascular enhancement pattern with a hyperechoic lesion relative to the surrounding normal parenchyma (Fig. 2A). Early washout and a hypoechoic lesion were observed in the portal phase (Fig. 2B), and an almost complete contrast defect was apparent in the Kupffer phase (Fig. 2C). The cystic regions within the nodule showed no internal enhancement in any phase.

In case 2, conventional abdominal US revealed an elliptical nodule with a well-defined margin in the central division of the liver (1.0 × 2.0 cm). The nodule showed a hyperechoic lesion and contained several small cystic regions (Fig. 3A–C). In CEUS, after the administration of contrast agent, the nodule showed a diffuse inhomogeneous enhancement pattern with a hypoechoic lesion and the surrounding liver parenchyma was also simultaneously enhanced in the arterial phase (Fig. 3A). The nodule then showed early washout and a hypoechoic lesion relative to the surrounding liver parenchyma in the portal phase (Fig. 3B) and a contrast defect in the Kupffer phase (Fig. 3C). The surrounding liver parenchyma in this dog histopathologically showed glycogen accumulation and was diagnosed as vacuolar hepatopathy.

In case 3, the dog had an elliptical nodule with a few small cystic regions in the right division of the liver (3.2 × 2.5 cm), which showed a hyperechoic lesion (Fig. 4A–C). In CEUS, a peripheral enhancement pattern (rim pattern) with isoechoic parenchyma was apparent in the arterial phase (Fig. 4A). The nodule showed early enhancement washout and a hypoechoic lesion relative to the surrounding normal parenchyma in the portal phase (Fig. 4B), as well as a complete contrast defect in the Kupffer phase (Fig. 4C). The cystic regions within the nodule showed no internal enhancement in any phase.

In veterinary medicine, CEUS with second-generation contrast agents, such as Definity[®] (Lantheus Medical Imaging, Inc., North Billerica, MA, U.S.A), SonoVue, and Sonazoid, are currently being used in clinical settings. Previous studies reported the usefulness of CEUS in terms of distinguishing malignant and benign liver tumors in dogs [8, 10, 12], as well as in humans [6, 11].

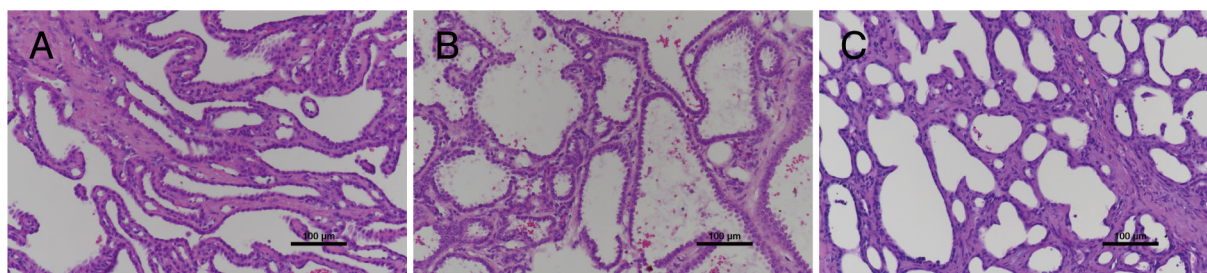


Fig. 1. Histopathologically, nodules in case 1 [A], case 2 [B] and case 3 [C] showed a ductular and papillary growth pattern and consisted well-differentiated cuboidal epithelium with cystic structures. These included no structures and cells derived from the hepatic parenchyma. Haematoxylin and eosin staining. Bars=100 μ m.

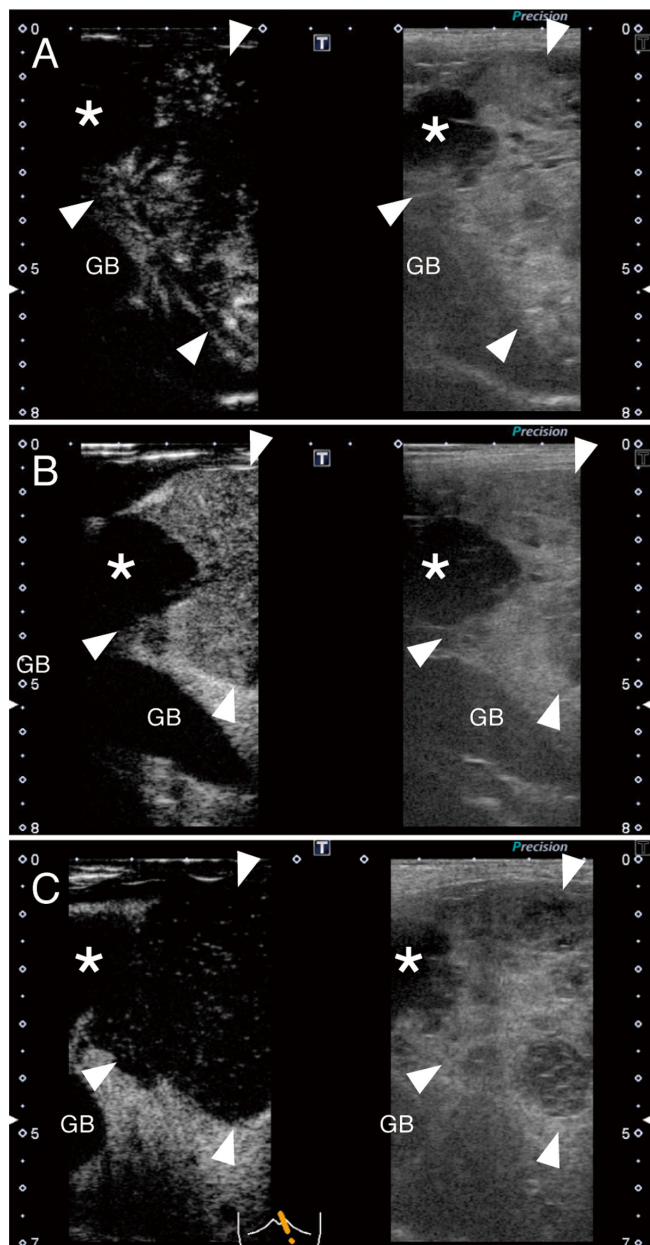


Fig. 2. Contrast-enhanced ultrasonography (left) and the conventional B-mode (right) images of the liver nodule in case 1. [A] Arterial phase image 3 sec after a bolus injection of Sonazoid. The nodule showed a dysmorphic vascular enhancement pattern with a hyperechoic lesion relative to the surrounding normal parenchyma. [B] Portal phase image 30 sec after a bolus injection of Sonazoid. The nodule showed a hypoechoic lesion relative to the surrounding normal parenchyma. [C] Kupffer phase image 7 min and 33 sec after a bolus injection of Sonazoid. The nodule showed a contrast defect. The cystic region (asterisks) was visible and showed no internal enhancement in any phase. Note the nodules (arrowheads) and the gall bladder (GB).

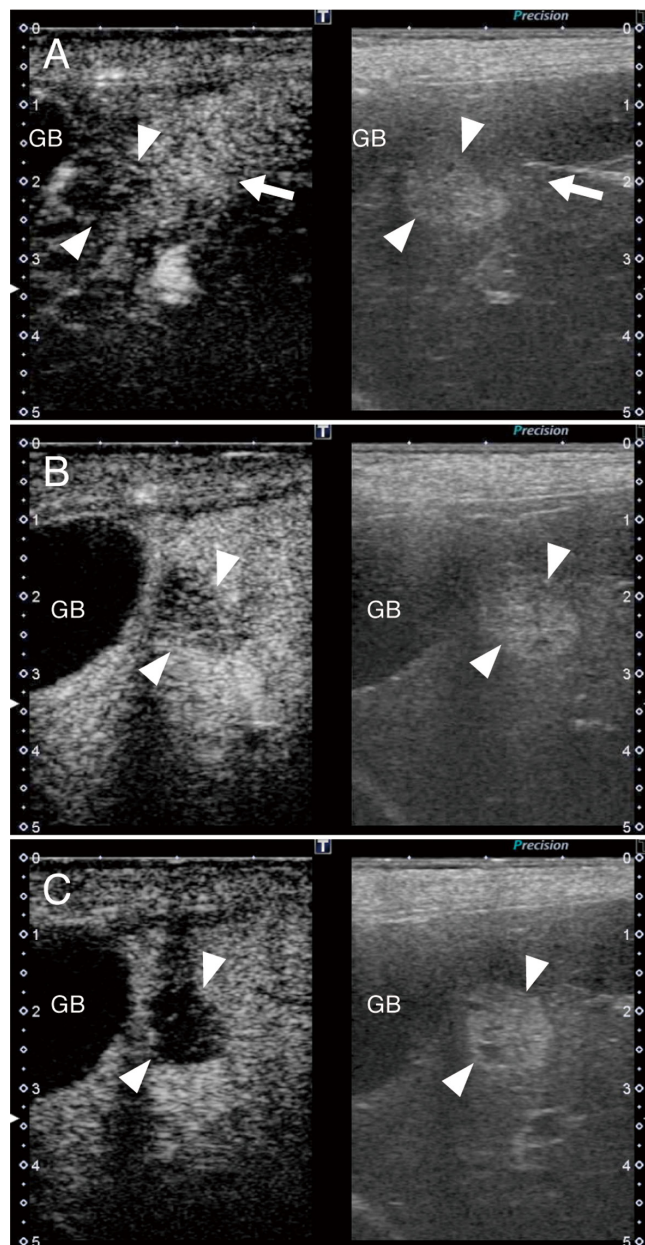


Fig. 3. Contrast-enhanced ultrasonography (left) and the conventional B-mode (right) images of the liver nodule in case 2. [A] Arterial phase image 5 sec after a bolus injection of Sonazoid. The nodule showed a diffuse inhomogeneous enhancement pattern with a hypoechoic lesion relative to the surrounding liver parenchyma that was simultaneously enhanced (arrow). [B] Portal phase image 30 sec after a bolus injection of Sonazoid. The nodule showed a hypoechoic lesion relative to the surrounding normal parenchyma. [C] Kupffer phase image 7 min and 35 sec after a bolus injection of Sonazoid. The nodule showed a contrast defect. Note the nodules (arrowheads) and the gall bladder (GB).

The findings of hypoechoic nodules at peak enhancement in the surrounding normal liver parenchyma using CEUS with Definity or SonoVue correlated with malignancy with very high sensitivity, specificity, positive predictive value, negative predictive value, and accuracy (100, 94.1, 93.8, 100, and 96.9%, respectively) [12]. However, this study did not include dogs with cholangiocellular adenoma. Baron *et al.* was the first to report that a dog with cholangiocellular adenoma showed findings mimicking malignant neoplasia on CEUS with SonoVue [1]. Moreover, findings mimicking malignancy in cholangiocellular adenoma on CEUS with

SonoVue were obtained in three human patients [7]; however, it was not reported whether CEUS with Sonazoid showed these findings.

In contrast to SonoVue, Sonazoid has the unique feature of accumulation in the reticuloendothelial system. Kupffer cells in the liver efficiently trap Sonazoid, resulting in the Kupffer phase, in addition to the vascular phase. Our research group using Sonazoid previously showed that 15 out of 16 dogs diagnosed with malignant liver nodules clearly had hypoechoic lesions relative to the surrounding normal parenchyma during the Kupffer phase [10]. Moreover, all six dogs diagnosed with benign nodular hyperplasia showed isoechoic parenchyma. Additionally, another study found that the sensitivity, specificity, positive predictive value, and negative predictive value of contrast defects in the Kupffer phase in malignant nodules were 100, 87.5, 93.8, and 100%, respectively (using Sonazoid) [8]. However, these two studies did not include dogs with cholangiocellular adenoma. Therefore, we retrospectively assessed the findings of CEUS with Sonazoid in three dogs diagnosed with cholangiocellular adenoma. All three dogs showed contrast defects during the Kupffer phase and findings which mimicked malignant neoplasia. However, the reason why cholangiocellular adenoma showed contrast defects during the Kupffer phase currently remains unknown. Cholangiocellular adenoma has an acinar, ductal, or papillary growth pattern and is composed of a large number of tubules lined by a well-differentiated, single layer cuboidal epithelium with cystic structures, with a normal liver parenchyma almost never being observed [3]. The mass in all our cases also had no structures or cells derived from the liver parenchyma. Findings mimicking malignancy in cholangiocellular adenoma may be caused by the absence of cells found in normal liver parenchyma, similar to a reduced number of Kupffer cells within malignant tumors. On the other hand, it is important that cyst, necrosis, or intranodular hemorrhage are also included a differential diagnosis if liver lesions show contrast defect. For example, congenital cystic diseases that are histologically similar to cholangiocellular adenoma show cyst of various sizes, which may be imaged as a nodule by conventional B-mode in spite of presenting with cystic structure histologically when cysts are too small. In fact, although case 2 was diagnosed as cholangiocellular adenoma and included cystic structure histologically, cystic regions was so small that it was a little difficult to recognize that in the conventional B-mode. Some tumors with extremely small cystic structure may also show contrast defect in the Kupffer phase. It is important to note that all liver lesions with cystic structure would show findings mimicking malignancy contrast defect by the absence of cells found in normal liver parenchyma.

In humans, evaluations of the vascular pattern of CEUS in the arterial phase are important in predicting different types of tumors. For example, hemangiomas frequently show globular enhancement in the peripheral area of a lesion in the arterial phase with progressive centripetal fill-in. The spoke-wheel pattern is a key finding for distinguishing focal nodular hyperplasia from high-flow hemangiomas, adenomas, and hypervascular malignant focal liver lesions [4]. However, vascular patterns to distinguish each tumor have not yet been established in veterinary medicine. Therefore, we assessed the CEUS findings of cholangiocellular adenoma in the arterial phase. However, nodules in the three dogs showed various patterns in the arterial phase: a dysmorphic vascular enhancement pattern with a hyperechoic lesion (case 1), a diffuse inhomogeneous enhancement pattern with a hypoechoic lesion (case 2), and a peripheral enhancement pattern

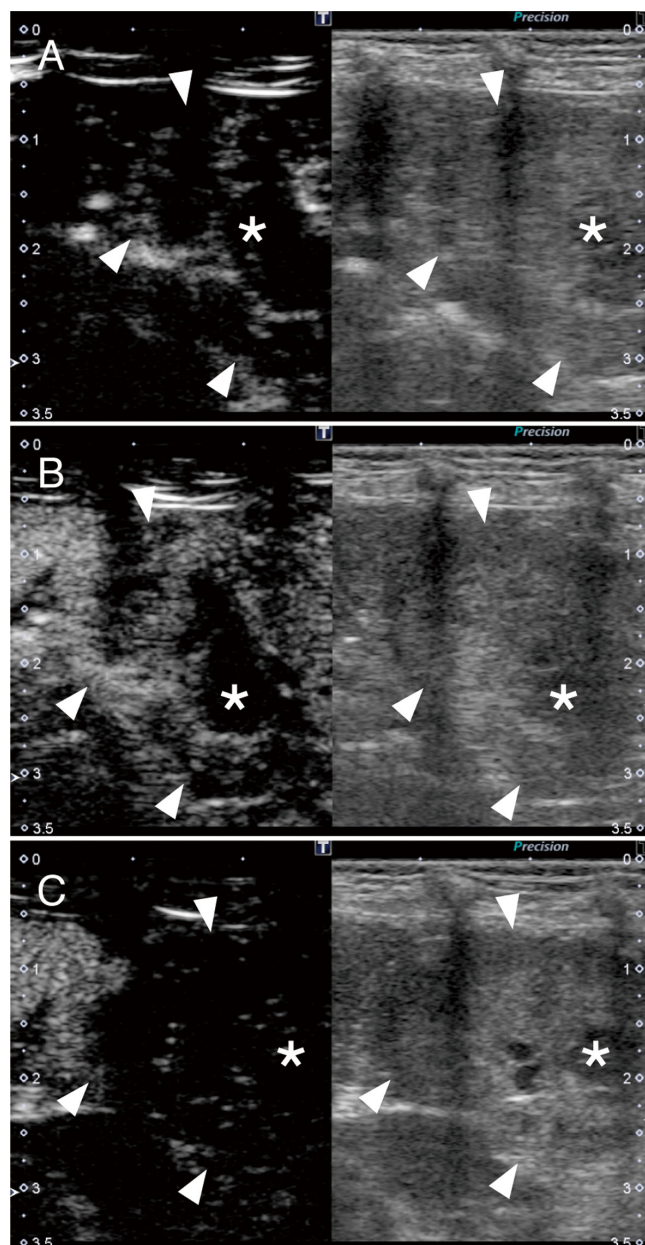


Fig. 4. Contrast-enhanced ultrasonography (left) and the conventional B-mode (right) images of the liver nodule in case 3. [A] Arterial phase image 3 sec after a bolus injection of Sonazoid. The nodule showed a peripheral enhancement pattern (rim pattern). [B] Portal phase image 30 sec after a bolus injection of Sonazoid. The nodule showed a hypoechoic lesion relative to the surrounding normal parenchyma. [C] Seven min after a bolus injection of Sonazoid. The nodule showed a contrast defect after the portal phase and Kupffer phase. The cystic region (asterisks) was visible and showed no internal enhancement in any phase. Note the nodules (arrowheads).

with an isoechoic lesion (case 3). Difficulties may be encountered to predict cholangiocellular adenoma based on the vascular pattern in the arterial phase.

We also evaluated CEUS findings in the portal phase in the present study, and found that all nodules showed early wash-out and hypoechoic lesions in this phase. Although the reason for this currently remains unknown, we assumed that (1) cholangiocellular adenoma is almost exclusively supplied from arterial blood flow and shows a decrease in portal vein blood flow or (2) cholangiocellular adenoma appears to be observed as a hypoechoic lesion because of a defect or decrease in Kupffer cells. However, since a previous study using SonoVue [1], which was not internalized in Kupffer cells, reported on the rapid washout after the peak enhancement of cholangiocellular adenoma in the arterial phase, which was similar to the present results; the former hypothesis may be conjectured. These hypotheses may be elucidated in the future using a quantified study with standardized protocols.

This study had several limitations. It was retrospective in nature and had a small number of cases. These cases may not represent the findings of the full spectrum of dogs with cholangiocellular adenoma. A prospective study with a larger population is needed in the future. Additionally, evaluation of the vascular patterns was only available in one section due to the short arterial phase. Hence, it was possible that a different vascular pattern in another section may be shown. Moreover, a quantitative CEUS parameter analysis of cholangiocellular adenoma was not performed in the present study because image acquisition was conducted by two investigators (M.T., K.N.) and the CEUS protocol was not identical among the dogs: the mechanical index and frame rate differed. These variables may have an impact on a quantitative analysis. Therefore, a quantified study comparing different types of tumors is needed to evaluate diagnostic accuracy for cholangiocellular adenoma.

To the best of our knowledge, this is the first study to report that CEUS findings of cholangiocellular adenoma with Sonazoid mimicked malignancy in three dogs, as reported previously using CEUS with SonoVue in a dog and humans with cholangiocellular adenoma. Cholangiocellular adenoma needs to be included in the differential diagnosis list for liver nodules even though it shows malignant findings on CEUS with Sonazoid.

ACKNOWLEDGMENTS. This work was supported in part by a Grant-in-Aid for JSPS Research Fellows (KAKENHI No. 18J21189) from the Japan Society for the Promotion of Science (M.T.). The authors wish to thank Dr. Yumiko Kagawa (Y.K.), an American College of Veterinary Pathologists board-certified pathologist, for her help with the interpretation of histopathological findings.

REFERENCES

1. Baron Toaldo, M., Diana, A., Bettini, G., Di Donato, P., Linta, N. and Cipone, M. 2013. Imaging diagnosis-cholangiocellular adenoma: contrast-enhanced ultrasonographic findings of a benign tumor mimicking malignant neoplasia in a dog. *Vet. Radiol. Ultrasound* **54**: 71–74. [[Medline](#)] [[CrossRef](#)]
2. Charles, J. A., Cullen, J. M., van den Ingh, T. S. G. A. M., Winkle, T. V. and Desmet, V. J. 2006. Morphological classification of neoplastic disorders of the canine and feline liver. pp. 117–124. *In: WSAVA Standards for Clinical and Histological Diagnosis of Canine and Feline Liver Diseases*, 1st ed. (WSAVA Liver Standardization Group eds.), Saunders Elsevier, Philadelphia.
3. Cullen, J. M. 2017. Tumors of the liver and gallbladder. pp. 602–631. *In: Tumors in Domestic Animals*, 5th ed. (Meuten, D. J. eds.), John Wiley & Sons, Ames.
4. D’Onofrio, M., Crosara, S., De Robertis, R., Canestrini, S. and Mucelli, R. P. 2015. Contrast-enhanced ultrasound of focal liver lesions. *AJR Am. J. Roentgenol.* **205**: W56–66. [[Medline](#)] [[CrossRef](#)]
5. Ferraioli, G. and Meloni, M. F. 2018. Contrast-enhanced ultrasonography of the liver using SonoVue. *Ultrasonography* **37**: 25–35. [[Medline](#)] [[CrossRef](#)]
6. Friedrich-Rust, M., Klopffleisch, T., Nierhoff, J., Herrmann, E., Vermehren, J., Schneider, M. D., Zeuzem, S. and Bojunga, J. 2013. Contrast-Enhanced Ultrasound for the differentiation of benign and malignant focal liver lesions: a meta-analysis. *Liver Int.* **33**: 739–755. [[Medline](#)] [[CrossRef](#)]
7. Ignee, A., Piscaglia, F., Ott, M., Salvatore, V. and Dietrich, C. F. 2009. A benign tumour of the liver mimicking malignant liver disease--cholangiocellular adenoma. *Scand. J. Gastroenterol.* **44**: 633–636. [[Medline](#)] [[CrossRef](#)]
8. Kanemoto, H., Ohno, K., Nakashima, K., Takahashi, M., Fujino, Y., Nishimura, R. and Tsujimoto, H. 2009. Characterization of canine focal liver lesions with contrast-enhanced ultrasound using a novel contrast agent-sonazoid. *Vet. Radiol. Ultrasound* **50**: 188–194. [[Medline](#)] [[CrossRef](#)]
9. Lim, S. Y., Nakamura, K., Morishita, K., Sasaki, N., Murakami, M., Osuga, T., Ohta, H., Yamasaki, M. and Takiguchi, M. 2013. Qualitative and quantitative contrast enhanced ultrasonography of the pancreas using bolus injection and continuous infusion methods in normal dogs. *J. Vet. Med. Sci.* **75**: 1601–1607. [[Medline](#)] [[CrossRef](#)]
10. Nakamura, K., Takagi, S., Sasaki, N., Bandula Kumara, W. R., Murakami, M., Ohta, H., Yamasaki, M. and Takiguchi, M. 2010. Contrast-enhanced ultrasonography for characterization of canine focal liver lesions. *Vet. Radiol. Ultrasound* **51**: 79–85. [[Medline](#)] [[CrossRef](#)]
11. Niu, Y., Huang, T., Lian, F. and Li, F. 2013. Contrast-enhanced ultrasonography for the diagnosis of small hepatocellular carcinoma: a meta-analysis and meta-regression analysis. *Tumour Biol.* **34**: 3667–3674. [[Medline](#)] [[CrossRef](#)]
12. O’Brien, R. T., Iani, M., Matheson, J., Delaney, F. and Young, K. 2004. Contrast harmonic ultrasound of spontaneous liver nodules in 32 dogs. *Vet. Radiol. Ultrasound* **45**: 547–553. [[Medline](#)] [[CrossRef](#)]
13. Sugimoto, K., Moriyasu, F., Saito, K., Taira, J., Saguchi, T., Yoshimura, N., Oshiro, H., Imai, Y. and Shiraishi, J. 2012. Comparison of Kupffer-phase Sonazoid-enhanced sonography and hepatobiliary-phase gadoxetic acid-enhanced magnetic resonance imaging of hepatocellular carcinoma and correlation with histologic grading. *J. Ultrasound Med.* **31**: 529–538. [[Medline](#)] [[CrossRef](#)]
14. Tang, M. X., Mulvana, H., Gauthier, T., Lim, A. K., Cosgrove, D. O., Eckersley, R. J. and Stride, E. 2011. Quantitative contrast-enhanced ultrasound imaging: a review of sources of variability. *Interface Focus* **1**: 520–539. [[Medline](#)] [[CrossRef](#)]